

Digital filters associated with bivariate box spline wavelets

Wenjie He

Ming-Jun Lai

University of Georgia

Department of Mathematics

Athens, Georgia 30602

E-mail: mjlai@math.uga.edu

Abstract. Battle-Lemarié's wavelet has a nice generalization in a bivariate setting. This generalization is called bivariate box spline wavelets. The magnitude of the filters associated with the bivariate box spline wavelets is shown to converge to an ideal high-pass filter when the degree of the bivariate box spline functions increases to ∞ . The passing and stopping bands of the ideal filter are dependent on the structure of the box spline function. Several possible ideal filters are shown. While these filters work for rectangularly sampled images, hexagonal box spline wavelets and filters are constructed to process hexagonally sampled images. The magnitude of the hexagonal filters converges to an ideal filter. Both convergences are shown to be exponentially fast. Finally, the computation and approximation of these filters are discussed. © 1997 SPIE and IS&T. [S1017-9909(97)00604-1]

1 Introduction

In recent papers,¹⁻³ the asymptotic properties of the filters associated with Daubechies' and Battle-Lemarié's wavelets have been studied. It was shown that the magnitude of the filters associated with Daubechies' wavelet and Battle-Lemarié's wavelet converges to an ideal filter. The Battle-Lemarié wavelet has a nice generalization in the bivariate setting, called the bivariate box spline wavelets (cf. Riemenschneider and Shen⁴). It is interesting to see the asymptotic properties of the filter associated with these bivariate wavelets. Since a bivariate box spline wavelet is not a tensor product of Battle-Lemarié's wavelets, the study of the asymptotic properties of bivariate box spline wavelet is not a simple generalization of the study carried out in Aldroubi and Unser.²

To be more precise about what we study in this paper, we have to introduce some necessary notation and definitions. Let $e_1 = (1, 0)$ and $e_2 = (0, 1)$ be the standard unit vectors in the Euclidean space \mathbf{R}^2 . A box spline over a three-direction mesh can be defined as follows. Let

$$B(x, y | e_1, e_2) = \begin{cases} 1, & (x, y) \in [0, 1]^2 \\ 0, & \text{otherwise,} \end{cases}$$

and inductively, assume that $B(x, y | X_m)$ is defined with direction set $X_m = \{x_1, \dots, x_m\}$, where x_i is one of three vectors e_1, e_2 , and $e_1 + e_2$, $i = 1, \dots, m$. For $X_m \cup \{x_{m+1}\}$,

$$B(x, y | X_m \cup x_{m+1}) = \int_0^1 B[(x, y) + t x_{m+1} | X_m] dt,$$

where x_{m+1} is e_1 or e_2 or $e_1 + e_2$.

For convenience, we consider the following box spline function in this paper:

$$B_{l,m,n}(x, y)$$

$$= B(x, y | \underbrace{e_1, \dots, e_1}_l, \underbrace{e_2, \dots, e_2}_m, \underbrace{e_1 + e_2, \dots, e_1 + e_2}_n).$$

Note that the Fourier transform of $B_{l,m,n}$ is

$$\hat{B}_{l,m,n}(\omega_1, \omega_2) = \left[\frac{1 - \exp(-j\omega_1)}{j\omega_1} \right]^l \left[\frac{1 - \exp(-j\omega_2)}{j\omega_2} \right]^m \times \left[\frac{1 - \exp[-j(\omega_1 + \omega_2)]}{j(\omega_1 + \omega_2)} \right]^n. \quad (1)$$

This expression resembles the Fourier transform of the well-known B -spline function. (For this and the other properties of box spline functions, see, e.g., Refs. 5 and 6. For computation with box spline functions, see Refs. 7 and 8.)

Furthermore, let $M_{l,m,n}(x, y) = B_{l,m,n}[(x, y) + c_{l,m,n}]$, with

$$c_{l,m,n} = [(l+n)/2, (m+n)/2],$$

where $M_{l,m,n}$ stands for the centered box spline function. The Fourier transform of $M_{l,m,n}$ is

$$\hat{M}_{l,m,n}(\omega_1, \omega_2) = [\text{sinc}(\omega_1/2)]^l [\text{sinc}(\omega_2/2)]^m \times [\text{sinc}(\omega_1 + \omega_2)/2]^n,$$

Paper IST-06 received Jan. 7, 1997; revised manuscript received Apr. 28, 1997; accepted for publication May 29, 1997. This paper is a revision of a paper presented at the SPIE conference on Wavelet Applications in Signal and Image Processing IV, Aug. 1996, Denver, CO. The paper presented there appears (unreferred) in SPIE Proceedings Vol. 2825. 1017-9909/97/\$10.00 © 1997 SPIE and IS&T.

where sinc is the sinc function, defined by $\text{sinc}(x) = \sin(x)/x$.

It is known that $B_n(x, y)$ generates a multiresolution approximation of $L^2(\mathbf{R}^2)$ (cf. Riemenschneider and Shen⁴). The Fourier transform of the scaling function $\psi_{(0,0)}$ is

$$\hat{\psi}_{(0,0)}^{(l,m,n)}(\omega_1, \omega_2) = \frac{\hat{B}_{l,m,n}(\omega_1, \omega_2)}{\{\sum_{(k_1, k_2) \in \mathbf{Z}^2} |\hat{M}_{l,m,n}[(\omega_1, \omega_2) + 2\pi(k_1, k_2)]|^2\}^{1/2}}. \quad (2)$$

Define a transfer function $H_{(0,0)}^{(l,m,n)}$, i.e., the Fourier transform of a digital filter by

$$H_{(0,0)}^{(l,m,n)}(\omega_1, \omega_2) = \frac{\hat{\psi}_{(0,0)}^{(l,m,n)}(2\omega_1, 2\omega_2)}{\hat{\psi}_{(0,0)}^{(l,m,n)}(\omega_1, \omega_2)}. \quad (3)$$

Then the wavelets $\psi_{\mathbf{k}}^{(l,m,n)}$, with $\mathbf{k} = \{(1,0), (0,1), (1,1)\}$ associated with the scaling function $\psi_{(0,0)}^{(l,m,n)}$ are given in terms of their Fourier transform by

$$\hat{\psi}_{\mathbf{k}}^{(l,m,n)}(\omega_1, \omega_2) = H_{\mathbf{k}}^{(l,m,n)}(\omega_1/2, \omega_2/2) \hat{\phi}_{(0,0)}^{(l,m,n)}(\omega_1/2, \omega_2/2). \quad (4)$$

Here, $H_{\mathbf{k}}^{(l,m,n)}$ is defined as follows:

$$H_{\mathbf{k}}^{(l,m,n)}(\omega_1, \omega_2) = \exp[j\omega \cdot \eta(\mathbf{k})] \times \begin{cases} H_{(0,0)}^{(l,m,n)}[(\omega_1, \omega_2) + \pi\mathbf{k}] & \text{if } c_{l,m,n} \text{ is an integer} \\ H_{(0,0)}^{(l,m,n)}[(\omega_1, \omega_2) + \pi\mathbf{k}] & \text{if } c_{l,m,n} \text{ is not an integer,} \end{cases}$$

where η is a mapping from $\Gamma_2 = \{(0,0), (1,0), (0,1), (1,1)\}$ to itself defined by

$$\eta[(0,0)] = (0,0), \eta[(1,0)] = (1,1), \eta[(0,1)] = (0,1), \eta[(1,1)] = (1,0),$$

(see, Riemenschneider and Shen⁴ for details).

Writing

$$H_{(0,0)}^{(l,m,n)}(\omega_1, \omega_2) = \sum_{(k_1, k_2) \in \mathbf{Z}^2} h_{k_1, k_2}^{(l,m,n)} \times \exp[-j(k_1\omega_1 + k_2\omega_2)],$$

we are interested in the properties and computations with digital filter $\{h_{k_1, k_2}^{(l,m,n)}, (k_1, k_2) \in \mathbf{Z}^2\}$. That is, we need to determine the passing and stopping bands of the digital filters for various choices of (l, m, n) . We show that the magnitude of the digital filters associated with $H_{(0,0)}^{(l,m,n)}$ converges to an ideal low-pass filter as $\nu \rightarrow +\infty$. Since

$$\sum_{\mathbf{k} \in \Gamma_2} |H_{\mathbf{k}}^{(l,m,n)}(\omega_1, \omega_2)|^2 = 1$$

(cf. Riemenschneider and Shen⁴), we can conclude that the digital filters associated with $H_{\mathbf{k}}^{(l,m,n)}$, $\mathbf{k} \in \Gamma_2 \setminus \{(0,0)\}$ converge to ideal high-pass filters as $\nu \rightarrow +\infty$.

Next, we note that those filters work only for rectangularly sampled digital images. For hexagonally sampled digital signals/images, we must construct hexagonal wavelets and therefore obtain hexagonal digital filters for processing these 2-D digital signals/images.⁹ Note that hexagonal sampling is the optimal sampling strategy for signals that are bandlimited over a circular region in the frequency domain (cf. Mersereau⁹) and is similar to what the human eyes are believed to do (cf. Watson and Ahumada¹⁰). See also Cohen and Schlenker¹¹ for another advantage that hexagonal filters possess in analyzing the image orientation. Thus, it is important for practical purposes to construct such hexagonal filters. It turns out that the construction can be adapted from that of box spline wavelets $\psi_{\mathbf{k}}^{(l,m,n)}$'s and transfer functions $H_{\mathbf{k}}^{(l,m,n)}$. Also, the asymptotic properties of the hexagonal filters are similar to those of the filters associated with $H_{\mathbf{k}}^{(l,m,n)}$. We deal with these hexagonal wavelets and filters in Sec. 3.

Finally, we discuss how to compute these filters numerically. We propose a matrix method to compute them. Although these filters are not finite impulse response (FIR) filters, they are of exponential decay, i.e.,

$$|h_{k_1, k_2}^{(l,m,n)}| \leq C \exp[-\alpha(|k_1| + |k_2|)], (k_1, k_2) \in \mathbf{Z}^2,$$

for some positive constants C and α . Thus, we can truncate the filter to be a reasonable FIR filter $\{h_{k_1, k_2}^{(l,m,n)}, |k_1| \leq N, |k_2| \leq N\}$ for some positive integer N . Furthermore, the FIR filter can be approximated using the singular value decomposition (SVD) method. That is, we can use the first few singular values and their singular vectors to approximate $\{h_{k_1, k_2}^{(l,m,n)}, |k_1| \leq N, |k_2| \leq N\}$. Then the processing of any 2-D signals/images with these singular values and vectors results a performance similar to that achieved when using tensor product of two 1-D digital filters. These are discussed in Sec. 4.

2 Asymptotic Properties of the Filters Associated with Box Spline Wavelets

We begin with the following lemmas. Let

$$a_{l,m,n}(\omega_1, \omega_2) = (\omega_1)^{2l} (\omega_2)^{2m} (\omega_1 + \omega_2)^{2n},$$

and

$$\Omega_{l,m,n} := \{(\omega_1, \omega_2) : a_{l,m,n}(\omega_1, \omega_2) < a_{l,m,n}(\omega_1 + 2\pi k_1, \omega_2 + 2\pi k_2), (k_1, k_2) \in \mathbf{Z}^2 \setminus (0,0)\}.$$

Lemma 1. The set $\Omega_{l,m,n}$ has a measure $4\pi^2$ and its integer translates $\Omega_{l,m,n} + 2\pi(k_1, k_2)$, $(k_1, k_2) \in \mathbf{Z}^2$ form an essential disjoint partition of \mathbf{R}^2 , i.e., (1) $\bar{\Omega}_{l,m,n} \cap [\Omega_{l,m,n} + 2\pi(k_1, k_2)] = \emptyset$, $(k_1, k_2) \in \mathbf{Z}^2 \setminus (0,0)$ and (2) the set $\mathbf{R}^2 \setminus \cup_{(k_1, k_2) \in \mathbf{Z}^2} [\Omega_{l,m,n} + 2\pi(k_1, k_2)]$ has a measure zero.

See de Boor and Höllig¹² for a proof. Next we have

Lemma 2. Function $|H_{(0,0)}^{(l,m,n)}(\omega_1, \omega_2)|^2$ is a periodic function with period $\bar{\Omega}_{l,m,n}$.

Proof. It is easy to see that $|H_{(0,0)}^{(l,m,n)}(\omega_1, \omega_2)|^2$ is a periodic function with period $[0, 2\pi]^2$. Now by using Lemma 1, we know that $\bar{\Omega}_{l,m,n}$ can serve as a period for $|H_{(0,0)}^{(l,m,n)}(\omega_1, \omega_2)|^2$. This completes the proof.

Note that $\Omega_{l,m,n} = \Omega_{l,m,n}$ for any $\nu > 0$. Let

$$\Omega_{l,m,n}^{ideal} := \{(\omega_1, \omega_2) : 2(\omega_1, \omega_2) \in \Omega_{l,m,n}\}.$$

We are now in a position to prove one of the main theorems in this paper.

Theorem 1. The magnitude of the digital filters whose Fourier transforms are $H_{(0,0)}^{(l,m,n,\nu)}$ converges to an ideal low-pass filter as $\nu \rightarrow \infty$. That is,

$$|H_{(0,0)}^{(l,m,n,\nu)}(\omega_1, \omega_2)| \rightarrow \begin{cases} 1, & (\omega_1, \omega_2) \in \Omega_{l,m,n}^{ideal} \\ 0, & (\omega_1, \omega_2) \in \Omega_{l,m,n} \setminus \bar{\Omega}_{l,m,n}^{ideal}. \end{cases}$$

Proof. From the definition of the scaling function $\hat{\psi}_{(0,0)}^{(l,m,n)}$, we can simplify $|\hat{\psi}_{(0,0)}^{(l,m,n)}|^2$ to get

$$\begin{aligned} & |\hat{\psi}_{(0,0)}^{(l,m,n)}(\omega_1, \omega_2)|^2 \\ &= \frac{1}{\left[1 + \sum_{\substack{(k_1, k_2) \neq (0,0) \\ (k_1, k_2) \in \mathbb{Z}^2}} \left[\frac{\omega_1}{\omega_1 + 2\pi k_1} \right]^{2l} \right]} \left[\frac{\omega_2}{\omega_2 + 2\pi k_1} \right]^{2m} \left[\frac{\omega_1 + \omega_2}{\omega_1 + \omega_2 + 2\pi(k_1 + k_2)} \right]^{2n} \\ &= \frac{1}{1 + \lambda_{l,m,n}(\omega_1, \omega_2)}. \end{aligned}$$

Thus, we have

$$\begin{aligned} |H_{(0,0)}^{(l,m,n)}(\omega_1, \omega_2)|^2 &= \frac{|\psi_{(0,0)}^{(l,m,n)}(2\omega_1, 2\omega_2)|^2}{|\psi_{(0,0)}^{(l,m,n)}(\omega_1, \omega_2)|^2} \\ &= \frac{1 + \lambda_{l,m,n}(\omega_1, \omega_2)}{1 + \lambda_{l,m,n}(2\omega_1, 2\omega_2)}. \end{aligned}$$

By Lemma 2, we consider only $(\omega_1, \omega_2) \in \Omega_{l,m,n}$. For $(\omega_1, \omega_2) \in \Omega_{l,m,n}^{ideal}$, we have both $\lambda_{l,m,n,\nu}(\omega_1, \omega_2) \rightarrow 0$ and $\lambda_{l,m,n,\nu}(2\omega_1, 2\omega_2) \rightarrow 0$ as $\nu \rightarrow \infty$. Thus,

$$|H_{(0,0)}^{(l,m,n,\nu)}(\omega_1, \omega_2)|^2 = \frac{1 + \lambda_{l,m,n,\nu}(\omega_1, \omega_2)}{1 + \lambda_{l,m,n,\nu}(2\omega_1, 2\omega_2)} \rightarrow 1.$$

For any $(\omega_1, \omega_2) \in \Omega_{l,m,n} \setminus \bar{\Omega}_{l,m,n}^{ideal}$, we have $\lambda_{l,m,n,\nu}(\omega_1, \omega_2) \rightarrow 0$. However, we have $\lambda_{l,m,n,\nu}(2\omega_1, 2\omega_2) \rightarrow +\infty$ as $\nu \rightarrow \infty$. Indeed, since $(2\omega_1, 2\omega_2) \notin \Omega_{l,m,n}$, there exists at least one integer $(k_1, k_2) \neq (0,0)$ such that

$$\begin{aligned} & \left[\frac{2\omega_1}{2\omega_1 + 2\pi k_1} \right]^{2l} \left[\frac{2\omega_2}{2\omega_2 + 2\pi k_2} \right]^{2m} \\ & \times \left\{ \frac{(2\omega_1 + 2\omega_2)}{[2\omega_1 + 2\omega_2 + 2\pi(k_1 + k_2)]} \right\}^{2n} > 1. \end{aligned}$$

It follows that

$$|H_{(0,0)}^{(l,m,n,\nu)}(\omega_1, \omega_2)|^2 \rightarrow 0.$$

Therefore, we have established the results of this theorem.

Certainly, the convergence of $|H_{(0,0)}^{(l,m,n,\nu)}(\omega_1, \omega_2)|$ is not uniform since the limit function is a discontinuous function. However, for each fixed $(\omega_1, \omega_2) \in \Omega_{l,m,n} \setminus \partial\Omega_{l,m,n}^{ideal}$, it converges to $\chi_{\Omega_{l,m,n}^{ideal}}(\omega_1, \omega_2)$ exponentially, where $\partial\Omega_{l,m,n}^{ideal}$ denotes the boundary of $\Omega_{l,m,n}^{ideal}$ and $\chi_{\Omega_{l,m,n}^{ideal}}$ is the characteristic function of $\Omega_{l,m,n}^{ideal}$. For example, for any $(\omega_1, \omega_2) \in \Omega_{l,m,n} \setminus \bar{\Omega}_{l,m,n}^{ideal}$, there exists (k_1, k_2) such that $a_{l,m,n}(2\omega_1, 2\omega_2) > a_{l,m,n}(2\omega_1 + 2\pi k_1, 2\omega_2 + 2\pi k_2)$, or

$$\left| \frac{\omega_1 + \pi k_1}{\omega_1} \right|^l \left| \frac{\omega_2 + \pi k_2}{\omega_2} \right|^m \left| \frac{\omega_1 + \omega_2 + \pi k_1 + \pi k_2}{\omega_1 + \omega_2} \right|^n < 1.$$

Note that we have

$$\begin{aligned} & ||H_{(0,0)}^{(l,m,n,\nu)}(\omega_1, \omega_1) - 0| \\ &= [|H_{(0,0)}^{(l,m,n,\nu)}(\omega_1, \omega_1)|^2]^{1/2} \\ &< \frac{[1 + \lambda_{l,m,n,\nu}(\omega_1, \omega_2)]^{1/2}}{\left(\frac{2\omega_1}{2\omega_1 + 2\pi k_1} \right)^{l\nu} \left(\frac{2\omega_2}{2\omega_2 + 2\pi k_2} \right)^{m\nu} \left[\frac{2\omega_1 + 2\omega_2}{2\omega_1 + 2\omega_2 + 2\pi(k_1 + k_2)} \right]^{n\nu}} \\ &= [1 + \lambda_{l,m,n,\nu}(\omega_1, \omega_2)]^{1/2} \\ &\times \left| \left(\frac{\omega_1 + \pi k_1}{\omega_1} \right)^l \left(\frac{\omega_2 + \pi k_2}{\omega_2} \right)^m \left(\frac{\omega_1 + \omega_2 + \pi k_1 + \pi k_2}{\omega_1 + \omega_2} \right)^n \right|^\nu. \end{aligned}$$

It follows from $\lambda_{l,m,n,\nu}(\omega_1, \omega_2) \rightarrow 0$ that $|H_{(0,0)}^{(l,m,n,\nu)}(\omega_1, \omega_1)|$ converges to zero pointwise exponentially fast. Similarly, for any $(\omega_1, \omega_2) \in \Omega_{l,m,n}^{ideal}$, we have

$$\begin{aligned} & ||H_{(0,0)}^{(l,m,n,\nu)}(\omega_1, \omega_1) - 1| \\ &\leq ||H_{(0,0)}^{(l,m,n,\nu)}(\omega_1, \omega_1)|^2 - 1| \\ &\leq \lambda_{l,m,n,\nu}(2\omega_1, 2\omega_2) + \lambda_{l,m,n,\nu}(\omega_1, \omega_2). \end{aligned}$$

Since $(\omega_1, \omega_2) \in \Omega_{l,m,n}$ and $(2\omega_1, 2\omega_2) \in \Omega_{l,m,n}$, there exists an integer N such that

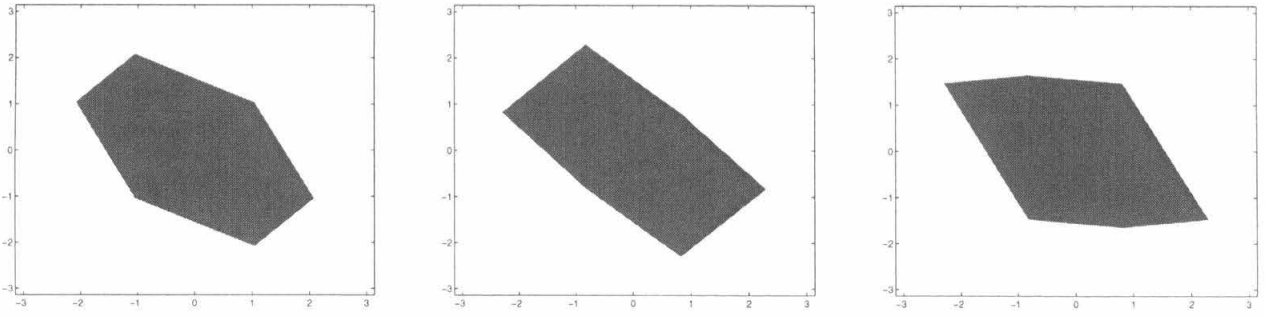


Fig. 1 Passing and stopping bands of some ideal low-pass filters for (1,1,1), (1,1,9), and (1,9,1).

$$\sum_{|k_1|+|k_2|\geq 2N} \left(\frac{\omega_1}{\omega_1+2\pi k_1}\right)^{2l\nu} \left(\frac{\omega_2}{\omega_2+2\pi k_2}\right)^{2m\nu}$$

$$\times \left[\frac{\omega_1+\omega_2}{\omega_1+\omega_2+2\pi(k_1+k_2)}\right]^{2n\nu}$$

$$\leq C \left[\left(\frac{\omega_1}{2\pi N-|\omega_1|}\right)^{2l\nu} + \left(\frac{\omega_2}{2\pi N-|\omega_2|}\right)^{2m\nu}\right],$$

and

$$\sum_{|k_1|+|k_2|\geq 2N} \left(\frac{\omega_1}{\omega_1+\pi k_1}\right)^{2l\nu} \left(\frac{\omega_2}{\omega_2+\pi k_2}\right)^{2m\nu}$$

$$\times \left[\frac{\omega_1+\omega_2}{\omega_1+\omega_2+\pi(k_1+k_2)}\right]^{2n\nu}$$

$$\leq C \left[\left(\frac{\omega_1}{\pi N-|\omega_1|}\right)^{2l\nu} + \left(\frac{\omega_2}{\pi N-|\omega_2|}\right)^{2m\nu}\right],$$

for some positive constant C . Thus, we have

$$\lambda_{l\nu,m\nu,n\nu}(\omega_1,\omega_2)$$

$$\leq \left(\sum_{\substack{|k_1|+|k_2|<2N \\ (k_1,k_2)\neq 0}} + \sum_{|k_1|+|k_2|\geq 2N}\right) \left(\frac{\omega_1}{\omega_1+2\pi k_1}\right)^{2l\nu}$$

$$\times \left(\frac{\omega_2}{\omega_2+2\pi k_2}\right)^{2m\nu} \left[\frac{\omega_1+\omega_2}{\omega_1+\omega_2+2\pi(k_1+k_2)}\right]^{2n\nu}$$

$$\leq \pi N^2 \left[\max_{\substack{|k_1|+|k_2|\leq N \\ (k_1,k_2)\neq(0,0)}} \frac{a_{l,m,n}(\omega_1,\omega_2)}{a_{l,m,n}(\omega_1+2\pi k_1,\omega_2+2\pi k_2)}\right]^\nu$$

$$+ C \left[\left(\frac{\omega_1}{2\pi N-|\omega_1|}\right)^{2l\nu} + \left(\frac{\omega_2}{2\pi N-|\omega_2|}\right)^{2m\nu}\right].$$

We have a similar estimate for $\lambda_{l\nu,m\nu,n\nu}(2\omega_1,2\omega_2)$. Thus, $|H_{(0,0)}^{(l\nu,m\nu,n\nu)}(\omega_1,\omega_1)|$ converges to 1 pointwise exponentially fast. Therefore, we can conclude the following.

Theorem 2. The magnitude of the filters associated with $H_{(0,0)}^{(l\nu,m\nu,n\nu)}$ converges to the ideal low-pass filter $\chi_{\Omega_{l,m,n}^i}$ pointwise exponentially fast.

In Figs. 1 and 2, we show $\Omega_{l,m,n}^{\text{ideal}}$ for some choices of (l,m,n) over $[-\pi,\pi]\times[-\pi,\pi]$. The passing bands are

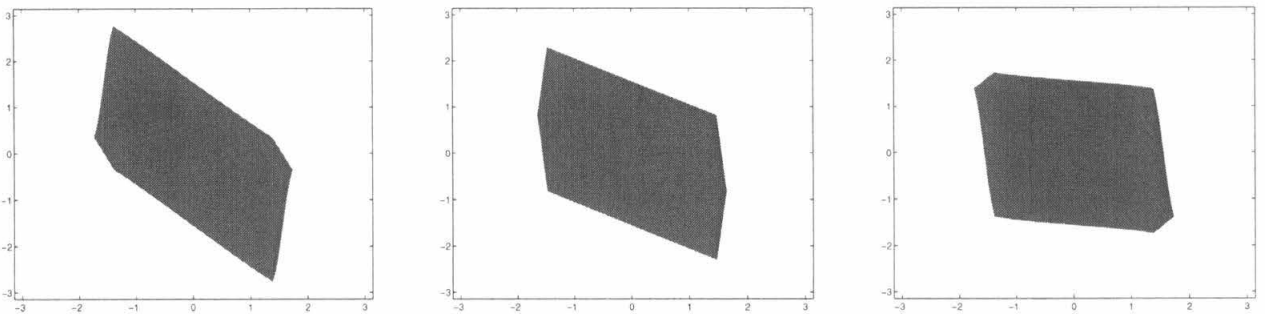


Fig. 2 Passing and stopping bands of some ideal low-pass filters for (9,1,9), (9,1,1), and (9,9,1).

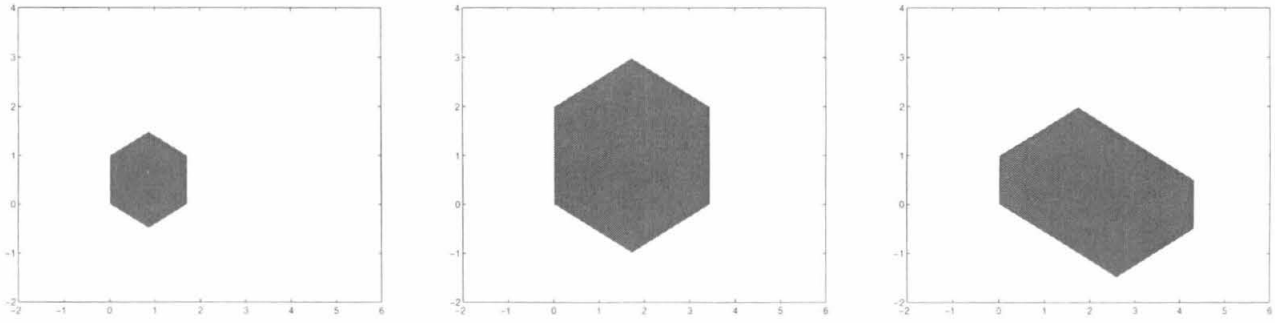


Fig. 3 Support of hexagonal box spline functions $B_{1,1,1}^\#$, $B_{2,2,2}^\#$, and $B_{1,2,3}^\#$.

of hexagonal shape with curve boundaries. For $(l,m,n) = (1,1,1)$, the hexagonal shape of the passing bands has piecewise linear boundaries.

3 Hexagonal Box Spline Wavelets and Filters

In this section, we construct hexagonal box spline wavelets and derive the filters that can be applied for hexagonally sampled signals/images. We start with hexagonal box splines, i.e., the box splines over a hexagonal grid $\{\mathbf{A}\mathbf{k}:\mathbf{k} \in \mathbb{Z}^2\}$ with

$$\mathbf{A} = \begin{bmatrix} \sqrt{3}/2 & 0 \\ 1/2 & 1 \end{bmatrix}$$

as in Simoncell and Adelson.¹³

For a direction set $X_n = \{\mathbf{x}^{(1)}, \dots, \mathbf{x}^{(n)}\}$, where $\mathbf{x}^{(i)}$ is one of $\mathbf{A}\mathbf{e}^{(1)}$, $\mathbf{A}\mathbf{e}^{(2)}$, $\mathbf{A}[e^{(1)} - e^{(2)}]$, $i = 1, \dots, n$, we define a hexagonal box spline $B^\#(x,y|X_n)$ inductively as follows. Rearranging, if necessary, such that

$$\begin{aligned} \text{area}([\mathbf{x}^{(1)}, \mathbf{x}^{(2)}]) \\ = \text{area}\{t_1\mathbf{x}^{(1)} + t_2\mathbf{x}^{(2)}, 0 < t_1 \leq 1, 0 < t_2 \leq 1\} > 0, \end{aligned}$$

we let

$$B^\#(x,y|\mathbf{x}^{(1)}, \mathbf{x}^{(2)}) = \begin{cases} 1/\text{area}([\mathbf{x}^{(1)}, \mathbf{x}^{(2)}]), & \text{if } (x,y) \in [\mathbf{x}^{(1)}, \mathbf{x}^{(2)}], \\ 0, & \text{otherwise,} \end{cases}$$

and for $m = 3, 4, \dots, n$, define

$$B^\#(x,y|\mathbf{x}^{(1)}, \dots, \mathbf{x}^{(m)}) = \int_0^1 B^\#[(x,y) - t\mathbf{x}^{(m)}|\mathbf{x}^{(1)}, \dots, \mathbf{x}^{(m-1)}] dt.$$

These box splines are of compact support. Let

$$Y_{l,m,n} = \underbrace{\{e^{(1)}, \dots, e^{(1)}\}}_l, \underbrace{\{e^{(2)}, \dots, e^{(2)}\}}_m, \underbrace{\{e^{(1)} - e^{(2)}, \dots, e^{(1)} - e^{(2)}\}}_n.$$

For convenience, let $B_{l,m,n}^\#(x,y) := B^\#(x,y|\mathbf{A}Y_{l,m,n})$. Then the support of some $B_{l,m,n}^\#$ is shown as in Fig. 3.

To understand these box spline functions better, we can quote the following basic result from de Boor *et al.*,⁵ which contains many more properties of these spline functions.

Lemma 3. For any continuous function f ,

$$\begin{aligned} \int_{\mathbb{R}^2} B^\#(x,y|X_n) f(x,y) dx dy \\ = \int_{[0,1]^n} f\left[\sum_{i=1}^n t_i \mathbf{x}^{(i)}\right] dt_1 \dots dt_n. \end{aligned}$$

These hexagonal box splines $B_{l,m,n}^\#$ are very much similar to box splines $B_{l,m,n}$. By letting $f(x,y) = \exp[-j(x\omega_1 + y\omega_2)]$ in Lemma 3, we have, letting $\omega = (\omega_1, \omega_2)^T$,

$$\begin{aligned} \hat{B}_{l,m,n}^\#(\omega_1, \omega_2) \\ = \left\{ \frac{1 - \exp[-je^{(1)}\mathbf{A}^T\omega]}{je^{(1)}\mathbf{A}^T\omega} \right\}^l \left\{ \frac{1 - \exp[-je^{(2)}\mathbf{A}^T\omega]}{je^{(1)}\mathbf{A}^T\omega} \right\}^m \\ \times \left(\frac{1 - \exp\{-j[e^{(1)} - e^{(2)}]\mathbf{A}^T\omega\}}{j[e^{(1)} - e^{(2)}]\mathbf{A}^T\omega} \right)^n. \end{aligned}$$

Furthermore, letting $\boldsymbol{\theta} = (\theta_1, \theta_2)^T = \mathbf{R}^{-1}\mathbf{A}^T\omega$,

$$\text{with } \mathbf{R} = \begin{bmatrix} 1 & 1 \\ 0 & 1 \end{bmatrix},$$

we have, by Eq. (1),

$$\hat{B}_{l,m,n}^\#(\mathbf{A}^{-T}\mathbf{R}\boldsymbol{\theta}) = \hat{B}_{n,m,l}(\theta_1, \theta_2). \tag{5}$$

Up to certain matrix transform, i.e., \mathbf{A} and \mathbf{R} , $B_{l,m,n}^\#$ is the same as $B_{n,m,l}$. All the construction of box splines wavelets based on $B_{l,m,n}$ can be easily adapted to the case of hexagonal box splines $B_{l,m,n}^\#$. For a complete exposition of the role of transforms \mathbf{A} and \mathbf{R} , we give a detail description of the construction of these hexagonal wavelets. Let

$$\mathcal{S}_{l,m,n} := \left\{ \sum_{\mathbf{k} \in \mathbf{Z}^2} c_{\mathbf{k}} B_{l,m,n}^{\#}[(x,y) - \mathbf{A}\mathbf{k}], \{c_{\mathbf{k}}\} \in \ell^2(\mathbf{Z}^2) \right\}$$

be the space of the hexagonal grid translates of a hexagonal box spline $B_{l,m,n}^{\#}$. Here, $\ell^2(\mathbf{Z}^2)$ denotes the space of all square summable sequences $\{c_{\mathbf{k}}\}$, i.e., $\sum_{\mathbf{k} \in \mathbf{Z}^2} |c_{\mathbf{k}}|^2 < \infty$. Then for any given hexagonally sampled digital signal/image $\{f(\mathbf{A}\mathbf{k}), \mathbf{k} \in \mathbf{Z}^2\}$ with a finite energy, there exists a unique spline interpolant $s_f := s_{f,l,m,n} \in \mathcal{S}_{l,m,n}$ such that

$$s_f(\mathbf{A}\mathbf{k}) = f(\mathbf{A}\mathbf{k}), \mathbf{k} \in \mathbf{Z}^2. \tag{6}$$

Multiplying Eq. (6) by $\exp(-j\omega\mathbf{A}\mathbf{k})$ and summing over \mathbf{k} , we get

$$\begin{aligned} \sum_{\mathbf{k} \in \mathbf{Z}^2} c_{\mathbf{k}} \exp(-j\omega\mathbf{A}\mathbf{k}) \sum_{\mathbf{k} \in \mathbf{Z}^2} B_{l,m,n}^{\#}(\mathbf{A}\mathbf{k}) \exp(-j\omega\mathbf{A}\mathbf{k}) \\ = \sum_{\mathbf{k} \in \mathbf{Z}^2} f(\mathbf{A}\mathbf{k}) \exp(-j\omega\mathbf{A}\mathbf{k}). \end{aligned}$$

Then the existence and uniqueness of such spline interpolant is guaranteed by the following lemma.

Lemma 4. For each integer (l,m,n) ,

$$\sum_{\mathbf{k} \in \mathbf{Z}^2} B_{l,m,n}^{\#}(\mathbf{A}\mathbf{k}) \exp(-j\omega\mathbf{A}\mathbf{k}) \neq 0, \forall \omega \in \mathbf{R}^2.$$

Proof. By Poisson's summation formula (cf. Ref. 14, p. 194), we have

$$\begin{aligned} \sum_{\mathbf{k} \in \mathbf{Z}^2} B_{l,m,n}^{\#}(\mathbf{A}\mathbf{k}) \exp(-j\omega\mathbf{A}\mathbf{k}) \\ = \frac{1}{\det(\mathbf{A})} \sum_{\mathbf{k} \in \mathbf{Z}^2} \hat{B}_{l,m,n}^{\#}(\omega - 2\pi\mathbf{A}^{-T}\mathbf{k}) \\ = \frac{1}{\det(\mathbf{A})} \sum_{\mathbf{k} \in \mathbf{Z}^2} \hat{B}_{l,m,n}^{\#}(\mathbf{A}^{-T}\mathbf{R}(\boldsymbol{\theta} - 2\pi\mathbf{R}^{-1}\mathbf{k})) \\ = \frac{1}{\det(\mathbf{A})} \sum_{\mathbf{k} \in \mathbf{Z}^2} \hat{B}_{n,m,l}^{\#}(\boldsymbol{\theta} - 2\pi\mathbf{k}) \neq 0 \end{aligned}$$

by Theorem 2 in de Boor *et al.*¹⁵ Here, we have used Eq. (3) and the fact that \mathbf{R}^{-1} is an integer matrix that is non-singular. This completes the proof.

In fact, we can further show that if an image is band limited in $\Omega_{l,m,n}^{\#}$ to be defined later in this section, $s_{f,l\nu,m\nu,n\nu}$ converges to f in L_2 norm as $\nu \rightarrow \infty$. We omit these details here. For similar results based on $B_{l,m,n}$ instead of $B_{l,m,n}^{\#}$, refer to de Boor *et al.*¹⁶

With this Lemma 4, we are able to prove the following.

Lemma 5. There exist two constants C_1 and C_2 such that

$$\begin{aligned} C_1 \sum_{\mathbf{k} \in \mathbf{Z}^2} |c_{\mathbf{k}}|^2 &\leq \int_{\mathbf{R}^2} \left| \sum_{\mathbf{k} \in \mathbf{Z}^2} c_{\mathbf{k}} B_{l,m,n}^{\#}[(x,y) - \mathbf{A}\mathbf{k}] \right|^2 dx dy \\ &\leq C_2 \sum_{\mathbf{k} \in \mathbf{Z}^2} |c_{\mathbf{k}}|^2, \end{aligned}$$

for any sequence $\{c_{\mathbf{k}}, \mathbf{k} \in \mathbf{Z}^2\} \in \ell^2(\mathbf{Z}^2)$.

Proof. We use Plancherel's theorem (cf. Ref. 14, p. 186) to get

$$\begin{aligned} (2\pi)^2 \int_{\mathbf{R}^2} \left| \sum_{\mathbf{k} \in \mathbf{Z}^2} c_{\mathbf{k}} B_{l,m,n}^{\#}[(x,y) - \mathbf{A}\mathbf{k}] \right|^2 dx dy \\ = \int_{\mathbf{R}^2} \left| \sum_{\mathbf{k} \in \mathbf{Z}^2} c_{\mathbf{k}} \exp(-j\omega\mathbf{A}\mathbf{k}) \hat{B}_{l,m,n}^{\#}(\omega) \right|^2 d\omega \\ = \int_{\mathbf{A}^{-T}[0,2\pi]^2} \left| \sum_{\mathbf{k} \in \mathbf{Z}^2} c_{\mathbf{k}} \exp(-j\omega\mathbf{A}\mathbf{k}) \right|^2 \sum_{\mathbf{k} \in \mathbf{Z}^2} |\hat{B}_{l,m,n}^{\#}(\omega - 2\pi\mathbf{A}^{-T}\mathbf{k})|^2 d\omega \\ = \int_{\mathbf{A}^{-T}[0,2\pi]^2} \left| \sum_{\mathbf{k} \in \mathbf{Z}^2} c_{\mathbf{k}} \exp(-j\omega\mathbf{A}\mathbf{k}) \right|^2 \\ \times \sum_{\mathbf{k} \in \mathbf{Z}^2} |\hat{B}_{2l,2m,2n}^{\#}(\omega + 2\pi\mathbf{A}^{-T}\mathbf{k})| d\omega. \end{aligned}$$

By Lemma 4, we have

$$C_1 = \min_{\omega \in [0,2\pi]^2} \sum_{\mathbf{k} \in \mathbf{Z}^2} \hat{B}_{2l,2m,2n}^{\#}(\omega + 2\pi\mathbf{A}^{-T}\mathbf{k}) > 0.$$

Letting $M_{l,m,n}^{\#}$ denote the centered hexagonal box spline as the centered box spline $M_{l,m,n}$ in Sec. 1, we have,

$$\begin{aligned} C_2 &= \max_{\omega \in \mathbf{A}^{-T}[0,2\pi]^2} \sum_{\mathbf{k} \in \mathbf{Z}^2} |\hat{B}_{2l,2m,2n}^{\#}(\omega + 2\pi\mathbf{A}^{-T}\mathbf{k})| \\ &= \max_{\omega \in \mathbf{A}^{-T}[0,2\pi]^2} \sum_{\mathbf{k} \in \mathbf{Z}^2} \hat{M}_{2l,2m,2n}^{\#}(\omega + 2\pi\mathbf{A}^{-T}\mathbf{k}) \\ &= \max_{\omega \in \mathbf{A}^{-T}[0,2\pi]^2} \sum_{\mathbf{k} \in \mathbf{Z}^2} M_{2l,2m,2n}^{\#}(\mathbf{A}\mathbf{k}) \exp(-j\omega\mathbf{A}\mathbf{k}) \\ &\leq \sum_{\mathbf{k} \in \mathbf{Z}^2} M_{2l,2m,2n}^{\#}(\mathbf{A}\mathbf{k}) = 1, \end{aligned}$$

using Poisson's summation formula, as in the proof of Lemma 4. This completes the proof.

With the preceding preparation, we are now able to define a multiresolution approximation of $L^2(\mathbf{R}^2)$ and construct hexagonal box spline wavelets. Let

$$V_k := \{f(2^k\mathbf{x}) : f(\mathbf{x}) \in \mathcal{S}_{l,m,n}\}, k \in \mathbf{Z}.$$

Then we have the following theorem.

theorem 3. The subspaces $V_k, k \in \mathbf{Z}$ form a multiresolution approximation of $L^2(\mathbf{R}^2)$. That is, they satisfy the following conditions:

1. $V_k \subset V_{k+1}, \forall k \in \mathbf{Z}$
2. $\forall f \in V_{k+1}, f(\mathbf{x}/2) \in V_k$ and $\forall k \in V_k, f(2\mathbf{x}) \in V_{k+1}, k \in \mathbf{Z}$
3. $\forall f \in V_k, f(\mathbf{x} - 2^{-k}\mathbf{A}\mathbf{i}) \in V_k, \forall \mathbf{i} \in \mathbf{Z}^2$
4. there exists a $\psi_0 \in V_0$ such that $\{\psi_0(\mathbf{x} - \mathbf{A}\mathbf{k}), \mathbf{k} \in \mathbf{Z}^2\}$ forms an orthonormal basis for V_0
5. $\cup_{k=-\infty}^{\infty} V_k$ is dense in $L^2(\mathbf{R}^2)$ and $\cap_{k=-\infty}^{\infty} V_k = \{0\}$.

The proof of Theorem 3 is similar to that in Riemenschneider and Shen.⁴ We omit the details. Note that condition 4 is equivalent to Lemma 5.

We are now in a position to define the scaling function $\psi_0^\#$ and wavelets $\psi_i^\#, i = 1, 2, 3$ associated with the multiresolution approximation $\{V_k\}$. Let

$$\begin{aligned} \psi_0^\#(\omega) &:= \widehat{\psi}_{0,(l,m,n)}^\#(\omega) \\ &= \frac{\widehat{B}_{l,m,n}^\#(\omega)[|\det(\mathbf{A})|]^{1/2}}{[\sum_{\mathbf{k} \in \mathbf{Z}^2} |\widehat{B}_{l,m,n}^\#(\omega + 2\pi\mathbf{A}^{-T}\mathbf{k})|^2]^{1/2}}. \end{aligned} \quad (7)$$

Then it is easy to check that $\psi_0^\#$, as defined, is in V_0 and satisfies the condition in the following lemma.

lemma 6. Suppose that $\phi \in L^2(\mathbf{R}^2)$. Then $\{\phi[(x,y) - \mathbf{A}\mathbf{k}], \mathbf{k} \in \mathbf{Z}^2\}$ is an orthonormal set if and only if

$$\sum_{\mathbf{i} \in \mathbf{Z}^2} |\hat{\phi}(\omega + 2\pi\mathbf{A}^{-T}\mathbf{k})|^2 = |\det(\mathbf{A})|, \quad \forall \omega \in \mathbf{R}^2.$$

The proof of this lemma is similar to the argument in the one-variable case. We again omit the details. Next we define the transfer functions

$$T_0^\#(\omega) = \frac{\hat{\psi}_0^\#(2\omega)}{\psi_0^\#(\omega)}, \quad (8)$$

and

$$T_i^\#(\omega) = \exp(j\omega^T \mathbf{s}_i) H_0^\#(\omega + \mathbf{t}_i), \quad i = 1, 2, 3, \quad (9)$$

with

$$\mathbf{t}_1 = \begin{bmatrix} \sqrt{3}/2 \\ 1/2 \end{bmatrix}, \quad \mathbf{s}_2 = \begin{bmatrix} 0 \\ 1 \end{bmatrix}, \quad \mathbf{s}_3 = \begin{bmatrix} -\sqrt{3}/2 \\ 1/2 \end{bmatrix},$$

and

$$\mathbf{t}_2 = \begin{bmatrix} 2\pi/\sqrt{3} \\ 0 \end{bmatrix}, \quad \mathbf{t}_3 = \begin{bmatrix} \pi/\sqrt{3} \\ \pi \end{bmatrix}, \quad \mathbf{t}_3 = \begin{bmatrix} \sqrt{3}\pi \\ \pi \end{bmatrix}.$$

Then the hexagonal box spline wavelets $\psi_i, i = 1, 2, 3$ can be defined in terms of Fourier transform as follows:

$$\psi_i(\omega) = H_i^\#(\omega/2) \hat{\psi}_0^\#(\omega/2), \quad i = 1, 2, 3. \quad (10)$$

To prove $\psi_i, i = 1, 2, 3$ are orthonormal wavelets, we need to prove the following lemmas, which are of independent interest.

Lemma 7. Functions $H_i^\#, i = 0, 1, 2, 3$ are a periodic function. That is,

$$H_i^\#(\omega + 2\pi\mathbf{A}^{-T}\mathbf{k}) = H_i^\#(\omega), \quad \forall \mathbf{k} \in \mathbf{Z}^2, \quad i = 0, 1, 2, 3.$$

Proof. Note that the denominator of $\hat{\psi}_0^\#$ and the numerator of $\hat{B}_{l,m,n}^\#$ are a periodic function. Observing that the denominator of $\hat{B}_{l,m,n}^\#$ in the expression of $\hat{\psi}_0^\#(2\omega)$ is canceled by that in $\hat{\psi}_0^\#(\omega)$ up to a factor of 2. We conclude that $H_0^\#$ is a such periodic function. Furthermore, since $\mathbf{s}_1 = \mathbf{A}e^{(1)}, \mathbf{s}_2 = \mathbf{A}e^{(2)}, \mathbf{s}_3 = \mathbf{A}[e^{(1)} - e^{(2)}]$, we know that $H_i^\#, i = 1, 2, 3$, are periodic functions:

Lemma 8. For $\omega \in \mathbf{R}^2$,

$$\sum_{\mathbf{k} \in \Gamma_2} |H_i^\#(\omega + \pi\mathbf{A}^{-T}\mathbf{k})|^2 = 1, \quad i = 0, 1, 2, 3.$$

Proof. By Lemma 6, we have

$$\begin{aligned} |\det(\mathbf{A})| &= \sum_{\mathbf{k} \in \mathbf{Z}^2} |\hat{\psi}_0^\#(\omega + 2\pi\mathbf{A}^{-T}\mathbf{k})|^2 \\ &= \sum_{\mathbf{k} \in \mathbf{Z}^2} |H_0^\#(\omega/2 + \pi\mathbf{A}^{-T}\mathbf{k}) \hat{\psi}_0^\#(\omega/2 + \pi\mathbf{A}^{-T}\mathbf{k})|^2 \\ &= \sum_{\mathbf{k} \in \mathbf{Z}^2} \sum_{\mathbf{i} \in \Gamma_2} |H_0^\#(\omega/2 + \pi\mathbf{A}^{-T}\mathbf{i})|^2 |\hat{\psi}_0^\#(\omega/2 + \pi\mathbf{A}^{-T}\mathbf{i} + 2\pi\mathbf{A}^{-T}\mathbf{k})|^2 \\ &= \sum_{\mathbf{i} \in \Gamma_2} |H_0^\#(\omega/2 + \pi\mathbf{A}^{-T}\mathbf{i})|^2 |\det(\mathbf{A})|. \end{aligned}$$

It follows that $\sum_{\mathbf{k} \in \Gamma_2} |H_i^\#(\omega + \pi\mathbf{A}^{-T}\mathbf{k})|^2 = 1, i = 1, 2, 3$.

Lemma 9. For $\mu, \nu \in \Gamma_2$ with $\mu \neq \nu$,

$$\sum_{\mathbf{k} \in \Gamma_2} H_\mu^\#(\omega + \pi\mathbf{A}^{-T}\mathbf{k}) \overline{H_\nu^\#(\omega + \pi\mathbf{A}^{-T}\mathbf{k})} = 0.$$

Proof. We can use Lemma 7 and the definition of $H_\mu^\#, \mu \in \Gamma_2$ to directly verify these identities. We omit these details.

We are now ready to show another main result in this paper.

Theorem 4. The functions $\psi_i^\#, i = 1, 2, 3$, as defined are wavelets. That is, the following collection of the dilations and translates of $\psi_i^\#$'s

$$\mathscr{W} := \{2^k \psi_i^\#[(2^k \mathbf{x} - \mathbf{A}\mathbf{j})], \mathbf{j} \in \mathbf{Z}^2, k \in \mathbf{Z}, i = 1, 2, 3\} \quad (11)$$

form an orthonormal basis of $L^2(\mathbf{R}^2)$.

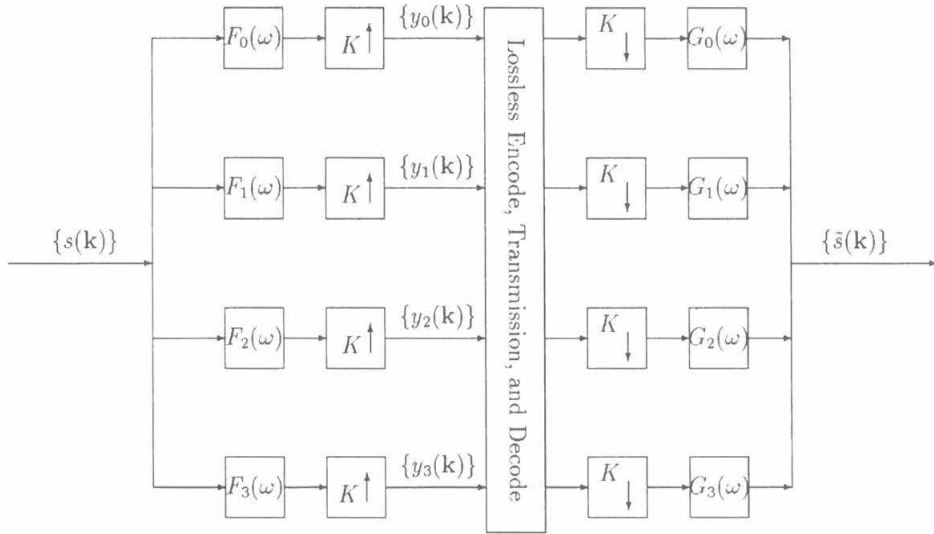


Fig. 4 Four-band analysis/synthesis filter bank.

Proof. The proof of this theorem is the same as in Riemenschneider and Shen.⁴ We omit the details.

Next we apply the hexagonal filters associated with $H_i^\#$, $i=0,1,2,3$ to subband coding design. Consider a 2-D four-band analysis synthesis filter bank (Fig. 4) as follows:

By choosing subsampling matrix

$$\mathbf{K} = \begin{bmatrix} 2 & 0 \\ 0 & 2 \end{bmatrix}$$

and filters

$$F_i(\omega) = \overline{G_i(\omega)} \exp(j\omega^T \cdot \mathbf{s}_i) H_{i0}^\#(\omega + \mathbf{t}_i), \quad i = 0, 1, 2, 3.$$

We can use Lemmas 6 and 9 to show that the Fourier transform \tilde{S} of the output image $\{\tilde{s}(\mathbf{k})\}$ is

$$\begin{aligned} \tilde{S}(\omega) &= \sum_{i=0}^3 G_i(\omega) Y_i(\mathbf{K}\omega) \\ &= \sum_{i=0}^3 G_i(\omega) \sum_{\mathbf{k}=0}^3 F_i(\omega + \mathbf{t}_\mathbf{k}) S(\omega + \mathbf{t}_\mathbf{k}) \\ &= \sum_{\mathbf{k}=0}^3 S(\omega + \mathbf{t}_\mathbf{k}) \sum_{i=0}^3 G_i(\omega) F_i(\omega + \mathbf{t}_\mathbf{k}) \\ &= S(\omega) \sum_{\mathbf{k}=0}^3 |H_{i0}^\#(\omega + \mathbf{t}_\mathbf{k})|^2 = S(\omega), \end{aligned}$$

which is the Fourier transform of the input image $\{s(\mathbf{k}), \mathbf{k} \in \mathbf{Z}^2\}$, where $Y_i(\omega)$ is the Fourier transform of digital filter $\{y_i(\mathbf{k})\}$, which is equal to

$$Y_i(\omega) = \sum_{\mathbf{k}=0}^3 F_i(\mathbf{K}^{-T}\omega + \mathbf{t}_\mathbf{k}) S(\mathbf{K}^{-T}\omega + \mathbf{t}_\mathbf{k}),$$

with

$$\mathbf{t}_0 = \pi \mathbf{A}^{-T} \begin{bmatrix} 0 \\ 0 \end{bmatrix}, \quad \mathbf{t}_1 = \pi \mathbf{A}^{-T} \begin{bmatrix} 1 \\ 0 \end{bmatrix},$$

$$\mathbf{t}_2 = \pi \mathbf{A}^{-T} \begin{bmatrix} 1 \\ 1 \end{bmatrix}, \quad \mathbf{t}_3 = \pi \mathbf{A}^{-T} \begin{bmatrix} 0 \\ 1 \end{bmatrix}$$

(cf. Simoncelli and Adelson¹³). Therefore, we have obtained the following.

Theorem 5. The filters whose Fourier transform are $H_i^\#$, $i=0,1,2,3$, respectively, form a subband filter bank with exact reconstruction.

Note that although the filters associated with $H_i^\#$'s are not FIR filters, they are of exponential decay. That is, writing

$$H_i^\#(\omega) = \sum_{\mathbf{k} \in \mathbf{Z}^2} h_{\mathbf{k}}^{[i]} \exp(-j\omega \mathbf{A} \mathbf{k}),$$

we know that

$$|h_{\mathbf{k}}^{[i]}| \leq C \exp[-\alpha(|k_1| + |k_2|)], \quad \mathbf{k} \in \mathbf{Z}^2,$$

for some positive constants C and α (cf. Corollary I). In the next section, we propose a computational method for these filters $\{h_{\mathbf{k}}^{[i]}, \mathbf{k} \in \mathbf{Z}^2\}$.

Finally, we consider the asymptotic behavior of these filters. Recall that $\psi_0^\# = \psi_{0,(l,m,n)}^\#$ and

$$H_{0,(l,m,n)}^\#(\omega) = \frac{\hat{\psi}_{0,(l,m,n)}^\#(2\omega)}{\hat{\psi}_{0,(l,m,n)}^\#(\omega)}.$$

For simplicity, let us consider $H_{0(v,v,v)}^\#$, which is the most important and interesting case since they converge to an ideal low-pass filter with a hexagonal passing band. Let

$$\Omega_{111}^\# := \{\omega: \mathbf{R}^{-1} \mathbf{A}^T \omega \in \Omega_{111}^{\text{deal}}\}.$$

Since Ω_{111}^0 is a hexagon with vertices

$$\left\{ \left(\frac{\pi}{3}, \frac{\pi}{3} \right), \left(-\frac{\pi}{3}, \frac{2\pi}{3} \right), \left(-\frac{2\pi}{3}, \frac{\pi}{3} \right), \left(-\frac{\pi}{3}, -\frac{\pi}{3} \right), \right. \\ \left. \left(\frac{\pi}{3}, -\frac{2\pi}{3} \right), \left(\frac{2\pi}{3}, -\frac{\pi}{3} \right) \right\},$$

so is $\Omega_{111}^\#$ with vertices

$$\left\{ \left(\frac{\pi}{\sqrt{3}}, \frac{\pi}{3} \right), \left(0, \frac{2\pi}{3} \right), \left(-\frac{\pi}{\sqrt{3}}, \frac{\pi}{3} \right), \left(-\frac{\pi}{\sqrt{3}}, -\frac{\pi}{3} \right), \right. \\ \left. \left(0, -\frac{2\pi}{3} \right), \left(\frac{\pi}{\sqrt{3}}, -\frac{\pi}{3} \right) \right\}.$$

We have the following.

Theorem 6. The filters whose Fourier transform are $H_{0,v}^\#$, $v=1,2,\dots$, converge to an ideal low-pass filter as $v \rightarrow \infty$. That is,

$$|H_{0,(v,v,v)}^\#(\omega)| \rightarrow \begin{cases} 1, & \text{if } \omega \in \Omega_{111}^\# \\ 0, & \text{if } \omega \in 2\Omega_{111}^\# \setminus \Omega_{111}^\# \end{cases}.$$

Proof. We note that

$$|H_{0,(v,v,v)}^\#(\mathbf{A}^{-T} \mathbf{R} \boldsymbol{\theta})|^2 = |H_{(0,0)}^{(v,v,v)}(\boldsymbol{\theta})|^2.$$

By Theorem 1, we conclude the result of this theorem.

4 Computation and Approximation of Box Spline Filters

We first recall from Sec. 1 that

$$H_{(0,0)}^{(l,m,n)}(\omega_1, \omega_2) \\ = \left[\frac{1 + \exp(-j\omega_1)}{2} \right]^l \left[\frac{1 + \exp(-j\omega_2)}{2} \right]^m \\ \times \left[\frac{1 + \exp[-j(\omega_1 + \omega_2)]}{2} \right]^n \\ \times \frac{\left\{ \sum_{(k_1, k_2) \in \mathbf{Z}^2} |\hat{M}_{l,m,n}[(2\omega_1, 2\omega_2) + 2\pi(k_1, k_2)]|^2 \right\}^{1/2}}{\left\{ \sum_{(k_1, k_2) \in \mathbf{Z}^2} |\hat{M}_{l,m,n}[(\omega_1, \omega_2) + 2\pi(k_1, k_2)]|^2 \right\}^{1/2}}.$$

By Poisson's summation formula as in Sec. 3, we have

$$\sum_{(k_1, k_2) \in \mathbf{Z}^2} |\hat{M}_{l,m,n}[(\omega_1, \omega_2) + 2\pi(k_1, k_2)]|^2 \\ = \sum_{(k_1, k_2) \in \mathbf{Z}^2} M_{2l,2m,2n}(k_1, k_2) \exp[-j(\omega_1 k_1 + \omega_2 k_2)].$$

That is, we are interested in computing coefficients $\{\alpha_{\mathbf{k}}\}_{\mathbf{k} \in \mathbf{Z}^2}$ and $\{\beta_{\mathbf{k}}\}_{\mathbf{k} \in \mathbf{Z}^2}$ in the following expansions

$$\left[\sum_{\mathbf{k} \in \mathbf{Z}^2} M_{2l,2m,2n}(\mathbf{k}) \exp(-j\mathbf{k} \cdot \boldsymbol{\omega}) \right]^{1/2} \\ = \sum_{\mathbf{k} \in \mathbf{Z}^2} \alpha_{\mathbf{k}} \exp(-j\mathbf{k} \cdot \boldsymbol{\omega}), \tag{12}$$

and

$$\frac{1}{\left[\sum_{\mathbf{k} \in \mathbf{Z}^2} M_{2l,2m,2n}(\mathbf{k}) \exp(-j2\mathbf{k} \cdot \boldsymbol{\omega}) \right]^{1/2}} \\ = \sum_{\mathbf{k} \in \mathbf{Z}^2} \beta_{\mathbf{k}} \exp(-j\mathbf{k} \cdot \boldsymbol{\omega}). \tag{13}$$

Let

$$P_{2l,2m,2n}(\omega_1, \omega_2) := \sum_{\mathbf{k} \in \mathbf{Z}^2} M_{2l,2m,2n}(\mathbf{k}) \exp(-j\mathbf{k} \cdot \boldsymbol{\omega}).$$

Note that $P_{2l,2m,2n}$ is a trigonometric polynomial. To compute the filter associated with $H_{(0,0)}^{(l,m,n)}$, we only need to compute the Fourier coefficients of $(P_{2l,2m,2n})^{1/2}$ and $1/(P_{2l,2m,2n})^{1/2}$.

We now describe a matrix method to do these computations. First of all, we consider bivariate banded and Toeplitz matrices $\mathbf{C} = (c_{\mathbf{i},\mathbf{j}})_{\mathbf{i},\mathbf{j} \in \mathbf{Z}^2}$. That is, \mathbf{C} is said to be bivariate banded if there exists a positive integer b such that $c_{\mathbf{i},\mathbf{j}} = 0$ whenever $|\mathbf{i} - \mathbf{j}| > b$, where $|\mathbf{i}| = |i_1| + |i_2|$ denotes the length of $\mathbf{i} = (i_1, i_2)$. Now \mathbf{C} is said to be a bivariate Toeplitz matrix if $c_{\mathbf{i}+\mathbf{k},\mathbf{j}+\mathbf{k}} = c_{\mathbf{i},\mathbf{j}}$ for all $\mathbf{i}, \mathbf{j}, \mathbf{k} \in \mathbf{Z}^2$. Denote by $F(\mathbf{C})(\boldsymbol{\omega})$ the symbol of a bivariate Toeplitz matrix $\mathbf{C} = (c_{\mathbf{i},\mathbf{j}})_{\mathbf{i},\mathbf{j} \in \mathbf{Z}^2}$, i.e.,

$$F(\mathbf{C})(\boldsymbol{\omega}) = \sum_{\mathbf{k} \in \mathbf{Z}^2} c_{\mathbf{k},(0,0)} \exp(-j\boldsymbol{\omega} \cdot \mathbf{k}).$$

Thus, $P_{2l,2m,2n}(\boldsymbol{\omega})$ is the symbol of the Toeplitz matrix $\mathbf{M}_{2l,2m,2n} = [M_{2l,2m,2n}(\mathbf{j} - \mathbf{i})]_{\mathbf{i},\mathbf{j} \in \mathbf{Z}^2}$. Similarly, $[\sum_{\mathbf{k} \in \mathbf{Z}^2} M_{2l,2m,2n}(\mathbf{k}) \exp(-j\mathbf{k} \cdot \boldsymbol{\omega})]^{1/2}$ can be viewed as the symbol of another (unknown) Toeplitz matrix $\mathbf{C}_{2l,2m,2n}$. Then it is easy to see that

$$\mathbf{C}_{2l,2m,2n}^2 = \mathbf{M}_{2l,2m,2n}.$$

Also, it is easy to see that the symbol of the bi-infinite matrix $\mathbf{C}^{-1}_{2l,2m,2n}$ is the trigonometric function $1/[\sum_{\mathbf{k} \in \mathbf{Z}^2} M_{2l,2m,2n}(\mathbf{k}) \exp(-j\mathbf{k} \cdot \boldsymbol{\omega})]^{1/2}$. Thus, to compute

		27	17	25	35			
		28	18	10	16	24	34	
	29	19	11	5	9	15	23	33
30	20	12	6	2	4	8	14	22
-13	-7	-3	-1	0	1	3	7	13
-22	-14	-8	-4	-2	-6	-12	-20	-30
-33	-23	-15	-9	-5	-11	-19	-29	
	-34	-24	-16	-10	-18	-28		
		-35	-25	-17	-27			

Fig. 5 Illustration of map $L(i, j)$.

α_k 's and β_k 's in Eqs. (12) and (13), it is equivalent to solve the correspondent matrices problems, i.e., matrix factorization and inversion.

Apparently we can not solve those infinite matrix factorizations and inversions. Our numerical method is to find their approximations. Let L be a one-one map from $\mathbf{Z}^2 \mapsto \mathbf{Z}$. For example, one of such maps of L can be defined as follows: writing $\mathbf{i}=(i_1, i_2) \in \mathbf{Z}^2$ and $n=|i_1|+|i_2|$, we define

$$L(\mathbf{i})=L(i_1, i_2) = \begin{cases} n(n-1)+i_2+1 & \text{if } i_1 \geq 0, i_2 \geq 0 \text{ but } n \neq 0 \\ n(n-1)+2n-i_2+1, & \text{if } i_1 < 0, i_2 > 0 \\ -n(n-1)-2n-i_2-1, & \text{if } i_1 \geq 0, i_2 < 0 \\ -n(n-1)+i_2-1, & \text{if } i_1 < 0, i_2 \leq 0 \\ 0 & \text{if } i_1=0, i_2=0 \end{cases}$$

This map L can be best illustrated by Fig. 5, where we let $L(0,0)=0$.

Then the bivariate bi-infinite matrix $\mathbf{M}_{2l,2m,2n}$ can be organized as a usual bi-infinite matrix

$$\mathbf{M}_{2l,2m,2n}=(b_{ij})_{i,j \in \mathbf{Z}},$$

with $b_{ij}=M_{2l,2m,2n}[L^{-1}(i)-L^{-1}(j)]$ for $i, j \in \mathbf{Z}$.

Let $\mathbf{M}_N=(b_{ij})_{-N \leq i, j \leq N}$ be a finite section of $\mathbf{M}_{2l,2m,2n}$. Note that \mathbf{M}_N is symmetric and positive definite. Thus we can find $\hat{\mathbf{P}}_N$ such that

$$\hat{\mathbf{P}}_N^2=\mathbf{M}_N,$$

by, e.g., SVD. Also, we can find the inverse $\hat{\mathbf{P}}_N^{-1}$ of $\hat{\mathbf{P}}_N$. We claim that $\hat{\mathbf{P}}_N$ converges to $\hat{\mathbf{C}}_{2l,2m,2n}$ and $\hat{\mathbf{P}}_N^{-1}$ to $\mathbf{C}_{2l,2m,2n}^{-1}$. That is, to approximate a bi-infinite matrix, we may use its finite sections.

To describe the convergence, we start with the following definition.

Definition 1. A matrix $\mathbf{A}=(a_{ij})_{i,j \in \mathbf{Z}}$ is said to be of bivariate exponential decay off its diagonal if

$$|a_{ij}| \leq Kr^{|L^{-1}(i)-L^{-1}(j)|},$$

for some constant K and $r \in (0,1)$.

Theorem 7. Let \mathbf{P} be the square root of a positive matrix \mathbf{A} . Suppose that \mathbf{A} is bivariate banded and $\|\mathbf{A}-I\|_2 \leq r < 1$, where I is the identity operator from $\mathcal{L}^2(\mathbf{Z}^2)$ to $\mathcal{L}^2(\mathbf{Z}^2)$. Then both \mathbf{P} and \mathbf{P}^{-1} are of bivariate exponential decay off its diagonal.

Proof. It is easy to see that

$$\begin{aligned} \mathbf{P} &= \sqrt{\mathbf{A}}=[I+(\mathbf{A}-I)]^{1/2} \\ &= \sum_{i=0}^{\infty} (-1)^i \frac{(2i-3)!!}{(2i)!!} (\mathbf{A}-I)^i, \end{aligned}$$

and

$$\begin{aligned} \mathbf{P}^{-1} &= (\mathbf{A})^{-1/2}=[I+(\mathbf{A}-I)]^{-1/2} \\ &= \sum_{i=0}^{\infty} (-1)^i \frac{(2i-1)!!}{(2i)!!} (\mathbf{A}-I)^i. \end{aligned}$$

It is also easy to understand that if $\mathbf{A}-I$ has bivariate bandwidth b , then $(\mathbf{A}-I)^k$ is also bivariate banded with bandwidth kb . Write $\mathbf{P}=(P_{ij})_{i,j \in \mathbf{Z}}$ and similarly for $(\mathbf{A}-I)^k$. We have, for $[|L^{-1}(i)-L^{-1}(j)|/b > n > |L^{-1}(i)-L^{-1}(j)|/b - 1$,

$$\begin{aligned} |P_{ij}| &= \left| \left[\sum_{k=n+1}^{\infty} (-1)^k \frac{(2k-3)!!}{(2k)!!} (\mathbf{A}-I)^k \right]_{ij} \right| \\ &\leq \sum_{k=n+1}^{\infty} \frac{(2k-3)!!}{(2k)!!} \|\mathbf{A}-I\|_2 \\ &\leq K_1 r^n \leq Kr^{|L^{-1}(i)-L^{-1}(j)|/b}, \end{aligned}$$

for some constant K . Therefore, \mathbf{P} is of exponential decay. Similarly, we can show that \mathbf{P}^{-1} is of exponential decay.

Corollary 1. The digital filter $\{h_{k_1, k_2}^{(l, m, n)}, (k_1, k_2) \in \mathbf{Z}^2\}$ associated with the transfer function $H_{(0,0)}^{(l, m, n)}$ is of exponential decay. That is,

$$|h_{k_1, k_2}^{(l, m, n)}| \leq C \exp(-\alpha[|k_1|+|k_2|]),$$

for some positive constants α and C .

Proof. Note that $H_{(0,0)}^{(l, m, n)}(\omega)$ is the symbol of a bivariate bi-infinite matrix $\mathbf{H}_{(l, m, n)}$, which is a product of three such matrices \mathbf{P} , $\mathbf{U}(\mathbf{P}^{-1})$, and \mathbf{J} , where $\mathbf{U}(\mathbf{P}^{-1})$ denotes the resulting bi-infinite matrix after upsampling of \mathbf{P}^{-1} by 2 and \mathbf{J} denotes the bi-infinite matrix whose symbol is

$$\left[\frac{1 + \exp(-j\omega_1)}{2} \right]^l \left[\frac{1 + \exp(-j\omega_2)}{2} \right]^m \times \left\{ \frac{1 + \exp[-j(\omega_1 + \omega_2)]}{2} \right\}^n.$$

Also, it is easy to see that $\mathbf{U}(\mathbf{P}^{-1})$ is of exponential decay. In fact, \mathbf{J} is a bivariate banded matrix and hence, of exponential decay. Since the family of bi-infinite matrices of exponential decay forms an algebra (cf. Ref. 17, p. 463), we conclude that $\mathbf{H}_{(l,m,n)}$ is of exponential decay and so is the digital filter $\{h_{k_1, k_2}^{(l,m,n)}\}$.

Theorem 8. Suppose that \mathbf{A} is a bivariate banded matrix satisfying the condition in Theorem 7. Let \mathbf{P} be the square root of \mathbf{A} and \mathbf{P}^{-1} be the inverse of \mathbf{P} . Let $\mathbf{A}_N, \mathbf{P}_N, \mathbf{P}_N^{-1}$ be a finite section of \mathbf{A}, \mathbf{P} , and \mathbf{P}^{-1} , respectively. Let $\hat{\mathbf{P}}_N$ be a square root matrix such that $\hat{\mathbf{P}}_N^2 = \mathbf{A}_N$ and $\delta_N = (0, \dots, 0, 1, 0, \dots, 0)^T$ be a vector of $2N + 1$ with zero entries except for the middle entry, which is 1. Then

$$\|\mathbf{P}_N \delta_N - \hat{\mathbf{P}}_N \delta_N\|_2 \leq K \eta^{\sqrt{N}},$$

and

$$\|\mathbf{P}_N^{-1} \delta_N - \hat{\mathbf{P}}_N^{-1} \delta_N\|_2 \leq K \eta^{\sqrt{N}},$$

for some $\eta \in (0, 1)$ and a positive constant K independent of N .

Proof. By the expression of \mathbf{P} in the proof of Theorem 7, we have

$$\|(\mathbf{P}_N - \hat{\mathbf{P}}_N) \delta_N\|_2 \leq \sum_{i=0}^{\infty} \frac{(2i-3)!!}{(2i)!!} \|\{[(\mathbf{A}-I)^i]_N - (\mathbf{A}_N - I_N)^i\} \delta_N\|_2.$$

We claim that

$$\|\{[(\mathbf{A}-I)^i]_N - (\mathbf{A}_N - I_N)^i\} \delta_N\|_2 \leq K \lambda^N,$$

for some $K > 0$ and $0 < \lambda \leq 1$. Let us use induction. For $i = 0$ and $i = 1$, it is clear that this estimate is true. Assume that this estimate is true for k . Consider

$$\begin{aligned} & [(\mathbf{A}-I)^{k+1}]_N - (\mathbf{A}_N - I_N)^{k+1} \\ &= [(\mathbf{A}-I)(\mathbf{A}-I)^k]_N - (\mathbf{A}-I)_N (\mathbf{A}_N - I_N)^k \\ &= [(\mathbf{A}-I)(\mathbf{A}-I)^k]_N - (\mathbf{A}-I)_N [(\mathbf{A}-I)^k]_N \\ &\quad + (\mathbf{A}-I)_N [(\mathbf{A}-I)^k]_N - (\mathbf{A}-I)_N (\mathbf{A}_N - I_N)^k. \end{aligned}$$

Note that

$$\begin{aligned} & \|\{(\mathbf{A}-I)_N [(\mathbf{A}-I)^k]_N - (\mathbf{A}-I)_N (\mathbf{A}_N - I_N)^k\} \delta_N\|_2 \\ & \leq \|\mathbf{A}-I\|_2 \|\{[(\mathbf{A}-I)^k]_N - (\mathbf{A}-I)_N (\mathbf{A}_N - I_N)^k\} \delta_N\|_2. \end{aligned}$$

We can use the induction hypothesis to take care of this part. Next we write

$$\mathbf{A}-I = \begin{bmatrix} \alpha_1 & \mathbf{B}'_N & \alpha_2 \\ \mathbf{B}_N & \mathbf{A}_N - I_N & \mathbf{C}_N \\ \alpha_3 & \mathbf{C}'_N & \alpha_4 \end{bmatrix}$$

and

$$(\mathbf{A}-I)^k = \begin{bmatrix} \beta_1 & \mathbf{a}_{N,k} & \beta_2 \\ \mathbf{a}'_{N,k} & [(\mathbf{A}-I)^k]_N & \mathbf{d}'_{N,k} \\ \beta_3 & \mathbf{d}_{N,k} & \beta_4 \end{bmatrix}.$$

Then we have

$$\begin{aligned} & [(\mathbf{A}-I)(\mathbf{A}-I)^k]_N - (\mathbf{A}-I)_N [(\mathbf{A}-I)^k]_N \\ &= \mathbf{B}_N \mathbf{a}_{N,k} + \mathbf{C}_N \mathbf{d}_{N,k}. \end{aligned}$$

Let us look closely at each component of the vector $(\mathbf{B}'_N \mathbf{a}_{N,k}) \delta_N$. That is, we look at the following terms, for $i = -N, \dots, 0, \dots, N$,

$$(\mathbf{B}_N \mathbf{a}_{N,k})_{i,0} = \sum_{\ell=-N+1}^{\infty} b_{i,\ell} a_{\ell,0},$$

with $\mathbf{B}_N = (b_{ij})$ and $\mathbf{a}_{N,k} = (a_{ij})$. Recall that $\mathbf{A}-I$ is bandwidth γ . If $k \gamma \leq N$, we know that $a_{\ell,0} = 0$ for all $\ell > N$. We have $(\mathbf{B}'_N \mathbf{a}_{N,k}) \delta_N = 0$. Similarly, we have $(\mathbf{C}_N \mathbf{d}_{N,k}) \delta_N = 0$. For $k > N/\gamma$, we simply have

$$\begin{aligned} & \|\{[(\mathbf{A}-I)(\mathbf{A}-I)^k]_N - (\mathbf{A}-I)_N [(\mathbf{A}-I)^k]_N\} \delta_N\|_2 \\ & \leq 2 \|(\mathbf{A}-I)^k\|_2 \leq r^k \leq r^{N/\gamma} = (r^\gamma)^N. \end{aligned}$$

Therefore, the claim is true for all k . Hence, we have

$$\|(\mathbf{P}_N - \hat{\mathbf{P}}_N) \delta_N\|_2 \leq \sum_{i=0}^{\infty} \frac{(2i-3)!!}{(2i)!!} K \lambda^N < K \lambda^N.$$

In the same fashion, we can show

$$\|(\mathbf{P}_N^{-1} - \hat{\mathbf{P}}_N^{-1}) \delta_N\|_2 \leq K \lambda^N.$$

We omit the details. This completes the proof.

To apply the preceding theorem, we therefore only need to verify that $\mathbf{M}_{2l, 2m, 2n}$ is a positive matrix and satisfies $\|\mathbf{M}_{2l, 2m, 2n} - I\|_2 < 1$. Indeed, letting $F(\mathbf{x})$ denote the Fourier transform of infinite vector $\mathbf{x} = \{x_i \mathbf{i} \in \mathbf{Z}^2\}$, i.e.,

$$F(\mathbf{x}) = \sum_{\mathbf{i} \in \mathbf{Z}^2} x_i \exp(-j \mathbf{i} \cdot \omega),$$

we have, by Parseval's equality,

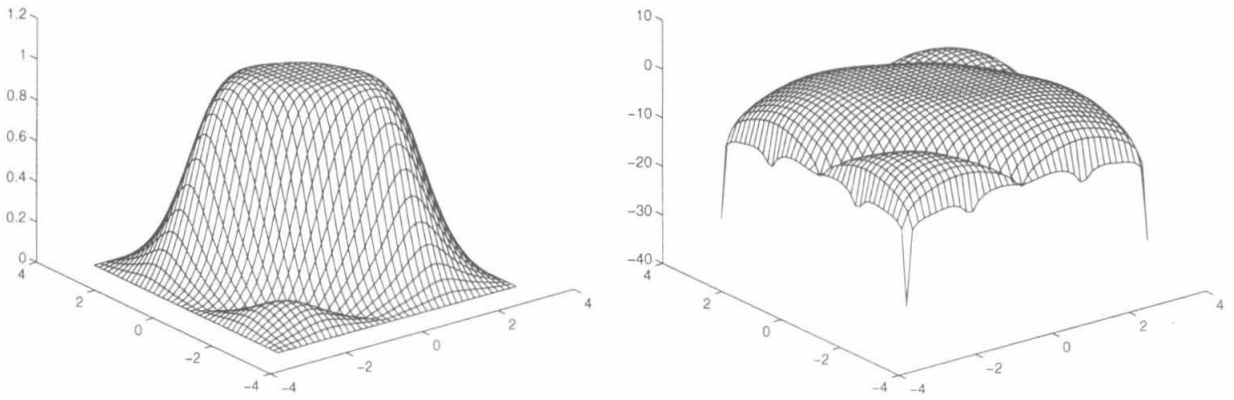


Fig. 6 Magnitude of low-pass filters $H_6^{(1,1,1)}$ and $\log_{10}(|H_6^{(1,1,1)}|^2)$.

$$\begin{aligned} \mathbf{x}^T \mathbf{M}_{2l,2m,2n} \mathbf{x} &= \frac{1}{(2\pi)^2} \int_{[-\pi, \pi]^2} \overline{F(\mathbf{x})} F(\mathbf{M}_{2l,2m,2n}(\omega)) \\ &\quad (\omega) F(\mathbf{x}) \, d\omega \\ &\geq \min_{\omega \in [-\pi, \pi]^2} F(\mathbf{M}_{2l,2m,2n})(\omega) \\ &\quad \times \frac{1}{(2\pi)^2} \int_{[-\pi, \pi]^2} |F(\mathbf{x})(\omega)|^2 \, d\omega \\ &= \min_{\omega \in [-\pi, \pi]^2} F(\mathbf{M}_{2l,2m,2n})(\omega) \|\mathbf{x}\|_2^2. \end{aligned}$$

$$\begin{aligned} \|(\mathbf{M}_{2l,2m,2n} - I)\mathbf{x}\|_2^2 &= \frac{1}{(2\pi)^2} \int_{[-\pi, \pi]^2} |F(\mathbf{M}_{2l,2m,2n} - I) \\ &\quad (\omega)|^2 |F(\mathbf{x})(\omega)|^2 \, d\omega \\ &= \frac{1}{(2\pi)^2} \int_{[-\pi, \pi]^2} |1 - F(\mathbf{M}_{2l,2m,2n}) \\ &\quad (\omega)|^2 |F(\mathbf{x})(\omega)|^2 \, d\omega \\ &\leq \max_{\omega \in [-\pi, \pi]^2} |1 - F(\mathbf{M}_{2l,2m,2n})(\omega)|^2 \|\mathbf{x}\|_2^2 \\ &\leq (1 - c)^2 \|\mathbf{x}\|_2^2. \end{aligned}$$

Since $c = \min_{\omega \in [-\pi, \pi]^2} F(\mathbf{M}_{2l,2m,2n})(\omega) > 0$ by Theorem 4 in de Boor *et al.*,¹⁵ we have $\mathbf{M}_{2l,2m,2n} \geq cI$. Using a similar method, we can show that $\|\mathbf{M}_{2l,2m,2n} - I\|_2 < 1$. Indeed,

Thus, $\mathbf{M}_{2l,2m,2n}$ satisfies all the conditions of Theorem 8.

Therefore, our numerical method provides a good approximation that converges the exact solution exponentially fast. In general, we are able to find a reasonable approximate $\mathbf{H}_N^{(l,m,n)} := \{h_{\mathbf{k}}^{l,m,n}\}_{|\mathbf{k}_1| \leq N, |\mathbf{k}_2| \leq N}$ with $N \leq 30$. See Figs. 6, 7, and 8 for $|\mathbf{H}_6^{(1,1,1)}|$, $|\mathbf{H}_{11}^{(2,2,2)}|$, and $|\mathbf{H}_{14}^{(3,3,3)}|$.

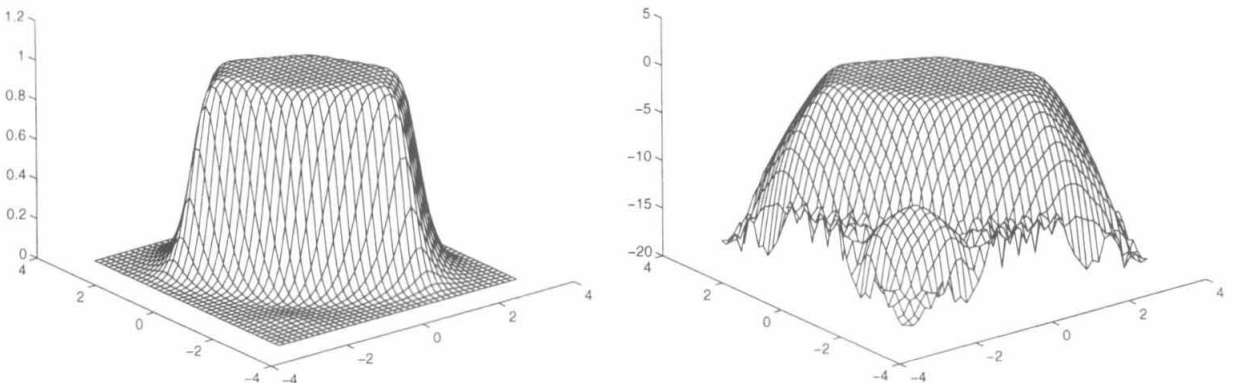


Fig. 7 Magnitude of low-pass filters $H_{11}^{(2,2,2)}$ and $\log_{10}(|H_{11}^{(2,2,2)}|^2)$.

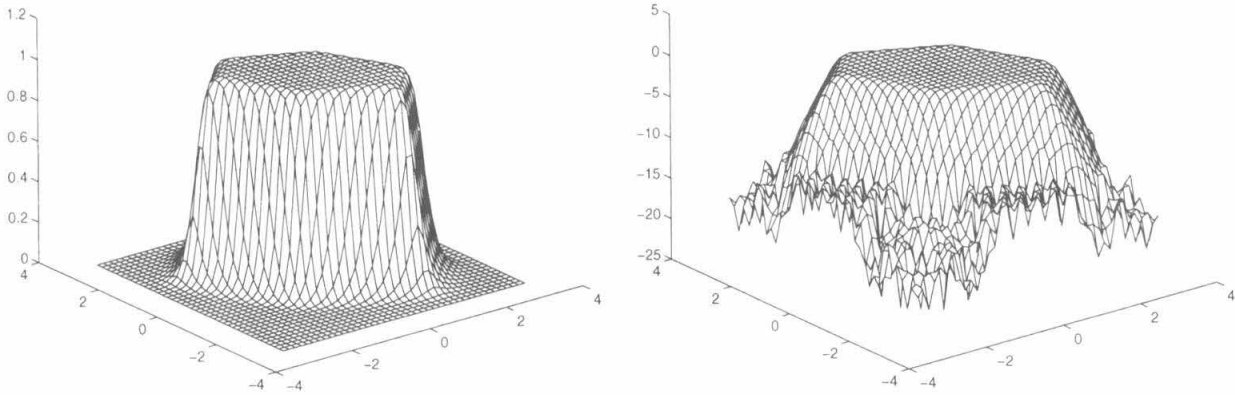


Fig. 8 Magnitude of low-pass filters $H_{14}^{(3,3,3)}$ and $\log_{10}(|H_{14}^{(3,3,3)}|^2)$.

For application purposes, the size of such filter matrices may still be too large. We now discuss how to approximate the filter matrix $\mathbf{H}_N^{(l,m,n)}$ by using SVD method. Note that $\mathbf{H}_N^{(l,m,n)}$ is a real matrix. Let

$$\mathbf{H}_N^{(l,m,n)} = \mathbf{U}^T \mathbf{\Sigma} \mathbf{V}$$

be the singular value decomposition of $\mathbf{H}_N^{(l,m,n)}$. Here, $\mathbf{U} = (\mathbf{u}_1 \dots \mathbf{u}_{2N+1})$ and $\mathbf{V} = (\mathbf{v}_1 \dots \mathbf{v}_{2N+1})$ are two orthonormal matrices and $\mathbf{\Sigma} = \text{diag}(\sigma_1, \dots, \sigma_{2N+1})$ is diagonal matrix with singular values σ_i 's on its diagonal. Let

$$\mathbf{H}_{N,\ell}^{(l,m,n)} = \sum_{i=1}^{\ell} \sigma_i \mathbf{u}_i \mathbf{v}_i^T$$

Then

$$\|\mathbf{H}_N^{(l,m,n)} - \mathbf{H}_{N,\ell}^{(l,m,n)}\|_2 = \min_{\text{rank}(\mathbf{G})=\ell} \|\mathbf{H}_N^{(l,m,n)} - \mathbf{G}\|_2 = \sigma_{\ell+1}$$

(Cf. e.g., Golub and Van Loan,¹⁸ p. 73.) Thus, we can determine ℓ from σ_i 's such that the approximation is within the given tolerance. Table 1 shows the first few singular values of $\mathbf{H}^{(l,m,n)}$ for $(l,m,n) = (1,1,1)$, $(2,2,2)$, and $(3,3,3)$.

Furthermore, when processing any 2-D digital signal/image \mathbf{S} with this filter $\mathbf{H}_{N,\ell}^{(l,m,n)}$, we immediately notice that

$$\mathbf{H}_{N,\ell}^{(l,m,n)} \star \mathbf{S} = \left(\sum_{i=1}^{\ell} \sigma_i \mathbf{u}_i \mathbf{v}_i^T \right) \star \mathbf{S} = \sum_{i=1}^{\ell} \sigma_i \mathbf{u}_i \star (\mathbf{v}_i^T \star \mathbf{S}),$$

where \star denotes the 2-D convolution operator. Because \mathbf{u}_i and \mathbf{v}_i are 1-D vectors, each term in the preceding summation is just a tensor-product filtering. Thus, the processing time using such a filter $\mathbf{H}_{N,\ell}^{(l,m,n)}$ is proportional to ℓ times that of a tensor-product filter. Therefore, these filters may be useful in practice.

References

1. N. Saito and G. Beyclin, "Multiresolution representation using the autocorrelation functions of compactly supported wavelets," *IEEE Trans. Signal Process.* **41**, 3584–3590 (1993).
2. A. Aldroubi and M. Unser, "Families of multiresolution and wavelet spaces with optimal properties," *Num. Funct. Anal. Optim.* **14**, 417–446 (1993).
3. M. J. Lai, "On the digital filter associated with Daubechies' wavelets," *IEEE Trans. Signal Process.* **43**, 2203–2205 (1995).
4. S. Riemenschneider and Z. Shen, "Box splines, cardinal series, and wavelets," in *Approximation Theory and Functional Analysis*, C. K. Chui, Ed., pp. 133–149, Academic Press, Boston (1991).
5. C. de Boor, K. Höllig, and S. Riemenschneider, *Box Splines*, Springer Verlag, New York (1993).
6. C. K. Chui, *Multivariate Splines*, SIAM Publications, Philadelphia (1988).
7. C. K. Chui and M. J. Lai, "Algorithms for generating B-nets and graphically displaying box spline surfaces," *Comput. Aided Geomet. Design* **8**, 479–493 (1992).
8. M. J. Lai, "Fortran subroutines for B-nets of box splines on three and four directional meshes," *Numer. Algorithm* **2**, 33–38 (1992).
9. R. Mersereau, "The processing of hexagonally sampled two-dimensional signals," *Proc. IEEE* **67**, 930–949 (1979).
10. A. Watson and A. Ahumada, Jr., "A hexagonal orthogonal-oriented pyramid as a model of image representation in visual cortex," *IEEE Trans. Biomed. Eng.* **36**, 97–106 (1989).
11. A. Cohen and J. M. Schlenker, "Compactly supported bidimensional wavelet bases with hexagonal symmetry," *Constr. Approx.* **9**, 209–236 (1993).
12. C. de Boor and K. Höllig, "Box-spline tilings," *Am. Math. Monthly* **98**, 793–802 (1991).
13. E. Simoncelli and E. H. Adelson, "Nonseparable extensions of quadrature mirror filters to multiple dimensions," *Proc. IEEE*, **78**, 652–664 (1990).
14. W. Rudin, *Real and Complex Analysis*, 3rd ed., McGraw-Hill, New York (1974).
15. C. de Boor, K. Höllig, and S. Riemenschneider, "Bivariate cardinal interpolation by splines on a three-direction mesh," *Ill. J. Math.* **29**, 533–566 (1985).
16. C. de Boor, K. Höllig, and S. Riemenschneider, "Convergence of cardinal series," *Proc. Am. Math. Soc.* **98**, 457–460 (1986).

Table 1 Some singular values of $\check{\mathbf{H}}^{(l,m,n)}$.

s Values	σ_1	σ_2	σ_3	σ_4	σ_5	σ_6
$H_6^{(1,1,1)}$	0.471	0.161	0.032	0.024	0.004	0.004
$H_{11}^{(2,2,2)}$	0.466	0.158	0.068	0.043	0.022	0.016
$H_{14}^{(3,3,3)}$	0.461	0.161	0.080	0.052	0.032	0.024
s Values	σ_7	σ_8	σ_9	σ_{10}	σ_{11}	σ_{12}
$H_6^{(1,1,1)}$	0.003	0.002	0.001	0.000	0.000	0.000
$H_{11}^{(2,2,2)}$	0.007	0.006	0.006	0.003	0.002	0.002
$H_{14}^{(3,3,3)}$	0.014	0.012	0.007	0.006	0.004	0.003

17. S. Jaffard, "Propriétés des matrices bien localisées près de leur diagonale et quelques applications," *Ann. Inst. Henri Poincaré* 7, 461–476 (1990).
18. G. H. Golub and C. F. Van Loan, *Matrix Computations*, Johns Hopkins University Press, Baltimore, MD (1989).



Wenjie He received a BS in mathematics from the Beijing University of China in 1988. He has been pursuing his doctoral studies in mathematics at the University of Georgia since 1992, and will graduate in 1998. His research interests are wavelets analysis and image processing.



Ming-Jun Lai received his PhD degree from the Department of Mathematics, Texas A&M University, in 1989, and has been an associate professor in the Department of Mathematics, the University of Georgia, Athens, since 1995. His research interests are approximation theory, computer-aided geometric design, multivariate splines, Navier-Stokes equations, numerical analysis, numerical solution of partial differential equations, signal and image processing, and wavelet analysis. He has published more than 30 papers in referred journals in these research areas.